2012 American Control Conference
Fairmont Queen Elizabeth, Montréal, Canada
June 27-June 29, 2012

State estimation in large-scale open channel networks using particle filters

Mohammad Rafiee*, Axel Barrau†, and Alexandre Bayen♭

*Department of Mechanical Engineering, University of California, Berkeley, CA, 94710-1740 USA

†Département de Mathématiques Appliquées, Ecole Polytechnique, Route de Saclay, 91128 Palaiseau Cedex, France

♭Department of Electrical Engineering and Computer Science and Department of Civil and Environmental Engineering, University of California, Berkeley, CA, 94720-1710 USA

Emails: rafiee@berkeley.edu, direction.etudes@polytechnique.fr, bayen@berkeley.edu

Abstract— **We consider the problem of estimating flow state in real time in large-scale open channel networks. After constructing a state space model of the flow based on the Saint-Venant equations, we implement the optimal *sequential importance resampling (SIR)* filter to perform state estimation using some additional flow measurements. The estimation method is implemented using a model of a network of 19 subchannels and one reservoir, Clifton Court Forebay, in Sacramento-San Joaquin Delta in California and the numerical results are presented.**

I. Introduction

Data assimilation is the process of integrating observations or measurements into a mathematical model of a physical system, in order to estimate some quantities of interest. Recently, data assimilation has provided rapid advances in geosciences such as meteorology, occeanography and hydrology [1], [3], [4], [21]. Different methods for assimilating data include variational data assimilation [5], filtering-based methods [15], [23], [28], [33], [31], [34], optimal statistical interpolation [27], or the Newtonian relaxation [18], [29].

Open channels are examples of the so-called *distributed parameter systems* in which the dynamics of the system can be modelled by a set of *partial differential equations (PDEs)*. For modelling the water flow in rivers and open channels, the Saint-Venant equations, which are a set of first-order hyperbolic nonlinear PDEs, are commonly used [11], [2]. Solving the PDEs requires an accurate knowledge of the boundary conditions, which are usually obtained from measurements of sensors installed at appropriate locations. Nevertheless, noise and inaccuracies in the measurements of the boundary conditions, as well as modelling assumptions (simplifications made to construct the mathematical model), can lead to mismatch between the values computed by the model and the actual state of the system. When additional observations (measurements) of the system are available, it is desirable to incorporate these measurements into the model to reduce the mismatch between the values computed by the model and the actual system throughout the whole domain of interest. Different state estimation methods can be used to estimate the state of the system in real time using available observations obtained from the system. In distributed parameters systems, where the system is typically high dimensional, it is important that state estimation methods with appropriate computational complexity are used so that real-time state estimation becomes tractable.

In the last decade, *sequential Monte Carlo methods*, also known as *Particle Filters* have attracted a lot of attention among researchers and practitioners due to their generality and scalability [16], [25], [7], [13], [14]. Particle filters can be applied to nonlinear systems and they do not require any Gaussianity assumptions on the noise. In particle filters, the posterior probability density function is approximated by a number of particles with their corresponding weights. These particles are propagated forward and their weights are updated at every time step. A larger number of particles results in more accurate results while it increases the computational cost of the method. Nonetheless, particle filters have shown to encounter different problems when implemented on various systems. The most critical issue observed in implementations of particle filters is the degeneracy problem [14]. When degeneracy happens, almost all of the particle weights vanish after a number of iterations meaning that most of the samples get too far from the actual state of the system and consequently they no longer contribute to approximating the posterior density function. Different methods have been developed to deal with the degeneracy problem among which *Sequential Importance Resampling (SIR)* filter is a most commonly used approach[22]. In the SIR filter, after each time step, the density function is resampled so that the samples with small weights are discarded and more probable samples are duplicated according to their weights.

In the current article, using one-dimensional Saint-Venant equations, we construct a state-space model of the flow in an open channel network. Considering a case where we have additional discharge measurements available at some locations in the network, our goal is to incorporate these measurements

into the model to improve the model results everywhere in the entire network. Given the observation model is linear and we assume the noises are Gaussian, we apply the optimal SIR filter to perform the data assimilation. We implement the method on a network of 19 subchannels and one reservoir in Sacramento-San Joaquin Delta in California.

The rest of this article is organized as follows: In section II, the one dimensional saint-Venant equations are presented and a state-space model of the flow in a network of open channels is constructed. In section III, we review the *optimal sequential resampling* (SIR) filter. Section IV provides information about the implementation of the method in a network of open channels in Sacramento-San Joaquin Delta in California and numerical results are presented. Finally, we conclude the article in section V.

II. Flow model

A. Saint-Venant Model

The Saint-Venant model is among the most common models used for modeling the flow in open channels and irrigation systems [11], [2]. In one dimensional case, Saint-Venant equations are two coupled first-order hyperbolic *partial differential equations* (PDEs) derived from conservation of mass and momentum. For prismatic channels with no lateral inflow, these equations can be written as follows [30]:

$$T\frac{\partial H}{\partial t}+\frac{\partial Q}{\partial x}=0 \tag{1}$$

$$\frac{\partial Q}{\partial t}+\frac{\partial}{\partial x}\left(\frac{Q^2}{A}\right)+\frac{\partial}{\partial x}(gh_cA)=gA(S_0-S_f) \tag{2}$$

for $(x,t)\in(0,L)\times\Re^+$, where L is the river reach (m), $Q(x,t)$ is the discharge or flow ($^{m^3}/_{s}$) across cross section $A(x,t)=T(x)H(x,t)$, $H(x,t)$ is the stage or water-depth (m), $T(x)$ is the free surface width (m), $D=A/T$ is the hydraulic depth (m), $S_f(x,t)$ is the friction slope ($^{m}/_{m}$), S_b is the bed slope ($^{m}/_{m}$), g is the gravitational acceleration ($^{m}/_{s^2}$) and h_c is the distance of the centroid of the cross section from the free surface (m).

The friction slope is empirically modelled by the Manning-Strickler's formula [24]:

$$S_f=\frac{m^2Q^2P^{4/3}}{A^{10/3}} \tag{3}$$

with $Q(x,t)=V(x,t)A(x,t)$ the discharge across cross-section $A(x,t)$, P the wetted perimeter, i.e. the perimeter of the wetted portion of the cross-section, and m the Manning's roughness coefficient ($sm^{-1/3}$).

In the case of sub-critical flow, the boundary conditions are taken to be upstream flow $Q(0,t)$ and downstream stage $H(L,t)$ or vice versa [24].

For channels with non-rectangular cross-sections, three correction parameters, α, η and γ can be introduced through the following equations, $A=\alpha TH$, $P=\eta(2T+H)$ and $h_c=\gamma H$. These parameters are calculated based on the average stage.

B. Discretization

We use the Lax diffusive scheme [10], [30] which is a first-order explicit scheme to discretize the equations at internal grid points. Using f to represent the state variables, Q and H, the derivatives become

$$\frac{\partial f}{\partial t}=\frac{f_i^{k+1}-\frac{1}{2}(f_{i+1}^k+f_{i-1}^k)}{\Delta t} \tag{4}$$

$$\frac{\partial f}{\partial x}=\frac{(f_{i+1}^k-f_{i-1}^k)}{2\Delta x} \tag{5}$$

using traditional finite difference discretization notation, with subscript i for space and superscript k for time.

Applying this scheme to equations (1) and (2), we obtain the following set of finite difference equations,

$$A_i^{k+1}=\frac{1}{2}(A_{i-1}^k+A_{i+1}^k)-\frac{\triangle t}{2\triangle x}(Q_{i+1}^k-Q_{i-1}^k) \tag{6}$$

$$Q_i^{k+1}=\frac{1}{2}(Q_{i-1}^k+Q_{i+1}^k)$$

$$-\frac{\triangle t}{2\triangle x}\left[\left(\frac{Q^2}{A}+gAh_c\right)_{i+1}^k-\left(\frac{Q^2}{A}+gAh_c\right)_{i-1}^k\right] \tag{7}$$

$$+\triangle t\left(\frac{\phi_{i+1}^k+\phi_{i-1}^k}{2}\right) \tag{8}$$

where

$$\phi=gA(S_b-S_f) \tag{9}$$

This scheme is stable provided that the *Courant-Friedrich-Lewy* (CFL) condition holds, i.e.

$$\frac{\Delta t}{\Delta x}|V+C|\leq 1 \tag{10}$$

where $C=\sqrt{gD}$ is the *wave celerity* and V is the average velocity.

However, the equations above may only be used for interior grid points. At the boundaries, these equations cannot be applied since there is no grid point outside the domain. Therefore, another method needs to be used to compute the unknown variables at the boundaries. Here, we use the ***method of specified time intervals*** to compute these variables [10]. In this method, after computing the characteristics, the boundary grid point is projected backward to the previous time step along its corresponding characteristic curve. After computing the variables at the projected point, which is usually done by using linear interpolation, the characteristic equations are used to compute the unknown variable at the boundary grid point at the next time step.

C. Internal Conditions for Confluence in Channel Network

In order to apply this model to a channel network, it is necessary to impose networked internal boundary conditions at every confluence in the channel network. Here, the internal boundary conditions constraints are briefly described for a

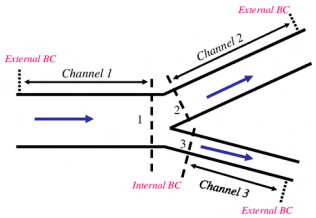

Fig. 1: Illustration of internal and external boundary conditions for a channel network.

simple confluence as in Figure 4 which comprises three channels. The constraints corresponding to the internal boundary conditions of stage and discharge are as follows:

$$H_1 = H_2 = H_3$$
$$Q_1 = Q_2 + Q_3$$

where H_1, H_2, and H_3 represent the stage in the cross sections 1, 2, and 3, respectively, and Q_1, Q_2, and Q_3 are the discharge at the three cross sections. The first equation is simply consistency of stage in all channels at the junction and the second equation is just the conservation of mass at the junction.

The discretized equations obtained from the Lax scheme and the method of specified time intervals along with the internal boundary constraints assembled to obtain a state-space model for the entire network of interest, written in a compact form as follows

$$x_{k+1} = f(x_k, u_k) \tag{11}$$

where x_k is the state vector at time k which consists of discharge and stage at all cells throughout the whole network excluding the external boundary condition variables, and the input vector u_k contains the external boundary conditions.

D. Stochastic State-space Model

The effect of modelling uncertainties, as well as inaccuracies in measurements of the inputs, are commonly considered as an additive noise term in the state equations (11) to obtain a stochastic equation

$$x_{k+1} = f(x_k, u_k) + v_k \tag{12}$$

The noise v_k is usually assumed to be zero-mean white Gaussian and

$$E[v_k v_l^T] = Q_k \delta_{kl} \tag{13}$$

$x_0 \in \mathbb{R}^m$ is the initial state which is also assumed to be Gaussian and

$$x_0 = \mathcal{N}(\bar{x}_0, P_0) \tag{14}$$

where $\bar{x}_0$ and P_0 are the initial guesses for state and error covariance.

Similarly, the errors and uncertainties in the measurements can be taken into account by adding a noise term to the measurement model to obtain

$$y_k = g(x_k, k) + e_k \tag{15}$$

where g is the function that relates the measurements to the state vector and e_k is the measurement noise of the sensors which is assumed to be zero-mean white Gaussian and

$$E[e_k e_l^T] = R_k \delta_{kl} \tag{16}$$

We also assume that the process and measurement noises and the initial conditions are all uncorrelated.

III. Optimal Sequential Importance Resampling Filter

In Bayesian estimation, the goal is to recursively calculate the conditional probability density function (pdf) $p(x_k|z_{1:k})$, where x_k is the state vector at time k and $z_{1:k}$ is the set of measurements obtained up to time step k. Assuming the initial state pdf $p(x_0)$ is known, the pdf $p(x_k|z_{1:k})$ may be calculated recursively in two steps, *prediction step* and *update step*. The prediction step uses the state-space model to propagate the conditional pdf forward in time. In other words, it calculates $p(x_k|z_{1:k-1})$ given $p(x_{k-1}|z_{1:k-1})$ via the Chapman-Kolmogorov equation

$$p(x_k|z_{1:k-1}) = \int p(x_k|x_{k-1}) p(x_{k-1}|z_{1:k-1}) dx_{k-1} \tag{17}$$

In the update step, when the measurements z_k becomes available, the conditional pdf is updated using the Bayes' rule

$$p(x_k|z_{1:k}) = \frac{p(z_k|x_k) p(x_k|z_{1:k-1})}{p(z_k|z_{1:k-1})} \tag{18}$$

where

$$p(z_k|z_{1:k-1}) = \int p(z_k|x_k) p(x_k|z_{1:k-1}) dx_k \tag{19}$$

While the above set of equations theoretically solve the Bayesian estimation problem, analytic solutions are tractable only in certain simplified cases, e.g. Kalman filter for linear systems with Gaussian noise [20]. For more general cases, different approximate solutions have been devised. Extended Kalman filters [6], approximate grid-based filters, unscented Kalman filters [19], [32], [17] and particle filters [13] are examples of these approximate methods.

Particle filtering is a sequential Monte Carlo method which calculates approximate solutions to the above equations for a general case of nonlinear systems with arbitrary process and measurement noises. The basic idea behind particle filters is that the posterior pdf $p(x_{0:k}|z_{1:k})$, where $x_{0:k} = \{x_j, j = 0, \cdots, k\}$ is the set of all state vectors up to time k, is approximated using a number of particles or random samples with their corresponding weights (probabilities). In other words

$$p(x_{0:k}|z_{1:k}) \approx \sum_{i=1}^{N_s} w_k^i \delta(x_{0:k} - x_{0:k}^i) \tag{20}$$

where $x^i_{0:k}$ is the i^{th} sample and w^i_k is its corresponding weight (the weights are normalized so they sum to one) and N_s is the number of samples. The estimates are computed using the particles and their associated weights and the weights are chosen using the principle of importance sampling [8].

A common problem with the sequential importance sampling particle filter is the degeneracy problem. However, a good choice of importance density can reduce the degeneracy of the particles. In this work, we choose the importance density $q(x_k|x^i_{k-1}, z_k)$ to be

$$\begin{aligned} q(x_k|x^i_{k-1}, z_k) &= p(x_k|x^i_{k-1}, z_k) \\ &= \frac{p(z_k|x_k, x^i_{k-1})p(x_k|x^i_{k-1})}{p(z_k|x^i_{k-1})} \end{aligned} \tag{21}$$

It has been shown [14] that this choice of importance density minimizes the variance of *true weights*, w^{*i}_k defined as $w^{*i}_k = p(x^i_k|z_{1:k})/q(x^i_k|x^i_{k-1}, z_k)$ which in turn maximizes the effective sample size defined as $N_{\text{eff}} = \dfrac{N_s}{1 + \text{Var}(w^{*i}_k)}$. We assume the process and measurement noises are mutually independent and independent identically distributed (i.i.d.) Gaussian and

$$v_{k-1} \sim \mathcal{N}(\mathbf{0}, Q_{k-1}) \tag{22}$$

$$e_{k-1} \sim \mathcal{N}(\mathbf{0}, R_{k-1}) \tag{23}$$

With this assumption, for systems with nonlinear dynamics and linear measurement model

$$x_k = f_k(x_{k-1}) + v_{k-1} \tag{24}$$

$$z_k = H_k x_k + e_k \tag{25}$$

it has been shown that $p(x_k|x^i_{k-1}, z_k)$ is Gaussian [14], [12] and

$$p(x_k|x_{k-1}, z_k) = \mathcal{N}(m_k, \Sigma_k) \tag{26}$$

$$p(z_k|x_{k-1}) = \mathcal{N}(H_k f_k(x_{k-1}), Q_{k-1} + H_k R_k H^T_k) \tag{27}$$

with

$$\Sigma^{-1}_k = Q^{-1}_{k-1} + H^T_k R^{-1}_k H_k \tag{28}$$

$$m_k = \Sigma_k(Q^{-1}_{k-1} f_k(x_{k-1}) + H^T_k R^{-1}_k z_k) \tag{29}$$

With this choice of importance density, the weights update equation simplifies to

$$w^i_k \propto w^i_{k-1} p(z_k|x^i_{k-1}) \tag{30}$$

$$= w^i_{k-1} \int p(z_k|x'_k) p(x'_k|x^i_{k-1}) dx'_k \tag{31}$$

In cases in which the degeneracy occurs even with this choice of importance density, resampling can be done whenever the effective sample size becomes too small [9]. In this resampling method, each particle generates a number of duplicates proportional to its weight and particles with small weights are discarded. A pseudo-code description of the resampling algorithm is provided in Algorithm 1.

Algorithm 1: Resampling Algorithm

$[\{x^{j*}_k, w^j_k, i^j\}^{N_s}_{j=1}] = \text{RESAMPLE}[\{x^i_k, w^i_k\}^{N_s}_{i=1}]$
Initialize the CDF: $c_1 = 0$
for $i = 2$ to N_s **do**
  Construct CDF: $c_i = c_{i-1} + w^i_k$
end for
Start at the bottom of the CDF: $i = 1$
Draw a starting point: $u_1 \sim \mathbb{U}[0, N^{-1}_s]$
for $j = 1$ to N_s **do**
  Move along the CDF: $u_j = u_1 + N^{-1}_s(j-1)$
  while $u_j > c_j$ **do**
    $i = i + 1$
  end while
  Assign sample: $x^{j*}_k = x^i_k$
  Assign weight: $w^j_k = N^{-1}_s$
  Assign parent: $i^j = i$
end for

Algorithm 2 illustrates particle filter with resampling

Algorithm 2: Particle filter with resampling

$[\{x^{j*}_k, w^j_k\}^{N_s}_{j=1}] = \text{PF}[\{x^i_{k-1}, w^i_{k-1}\}^{N_s}_{i=1}, z_k]$
for $i = 1$ to N_s **do**
  Draw $x^i_k \sim q(x_k|x^i_{k-1}, z_k) = p(x_k|x^i_{k-1}, z_k)$
  Assign the particle a weight, w^i_k, using (31).
end for
Calculate total weight: $t = \sum^{N_s}_{i=1} w^i_k$
for $i = 1$ to N_s **do**
  Normalize: $w^i_k = t^{-1} w^i_k$
end for
Calculate $\hat{N}_{\text{eff}} = \dfrac{1}{\sum^{N_s}_{i=1}(w^i_k)^2}$
if $\hat{N}_{\text{eff}} < N_T$ **then**
  Resample using algorithm 1:
  $[\{x^i_k, w^i_k, -\}^{N_s}_{i=1}] = \text{RESAMPLE}[\{x^i_k, w^i_k\}^{N_s}_{i=1}]$
end if

IV. Implementation

We consider a network of 19 subchannels and one reservoir in the southern part of Sacramento-San Joaquin to implement the data assimilation methods. The Sacramento-San Joaquin Delta, in northern California, is the hub of California's water system. This complex network covers 738,000 acres interlaced with over 1150 km of tidally influenced channels and sloughs and approximately 50 percent of California's average annual streamflow flows to the Delta. Figure 3 shows a map of the Delta.

TABLE I: The names and geometry information of the subchannels in the open channel network in Sacarameto-San Joaquin Delta in California used for the implementations.

Channel	River	Length	Avg. width	Avg. depth
1-2	Italian Slough	14198	234.0	14.0
2-3	Italian Slough	2723	203.4	16.4
2-5	Italian Slough	3227	437.5	10.3
3-4	Old River	4754	351.3	21.8
3-5	Old River	5022	351.2	22.0
5-6	Old River	4313	238.4	13.0
5-11	West Canal	10041	253.0	28.0
6-7	Victoria Canal	8760	386.5	18.3
6-8	Old River	2722	276.3	15.2
8-9	Old River	2793	109.0	11.7
8a9	Old River	5347	157.1	9.0
9-10	Old River	2456	109.0	11.7
9a10	Old River	5062	157.1	9.0
10-11	Old River	7744	198.4	12.4
11-13	Old River	2609	266.0	19.0
13-14	Old River	3857	245.0	17.8
14-16	Old River	12089	176.0	10.0
14-15	Mendota Canal	12500	196.0	18.0
13-17	Grant Line Canal	15831	404.0	16.0

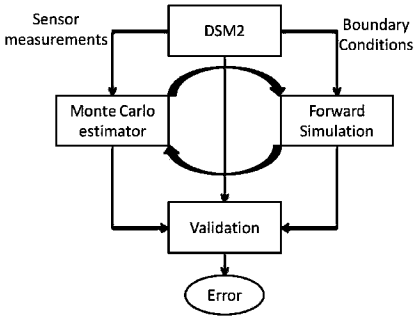

Fig. 2: A flow diagram of the experiment.

The network considered for implementation consists of the Clifton Court Forebay and its surrounding channels which are parts of the Old River, the Italian Slough, the Mendota Canal, the West Canal, the Victoria Canal and the Grant Line Canal and is located on the northern side of Tracy. Figure 4 shows a satellite picture of the area and a map of the network with the channel configuration of the network, considered in building a one-dimensional model of the flow. As can be seen in this figure, this network consists of one reservoir, 19 subchannels and 10 junctions. The total length of the channels in the network is 38,420 m. Table I presents the name and some geometry information about the channels. The channels are represented by their parent nodes from figure 4.

Figure 2 shows a flow diagram of the experiment. We use the Delta Simulation Model II, DSM2, to obtain measurements for boundary conditions and data assimilation as well as to evaluate our results. DSM2 is a one dimensional mathematical model, developed in the California *Department of Water Resources* (DWR), for dynamic simulation of hydrodynamics, water quality and particle tracking in the Delta. DSM2 can calculate stages, flows, velocities, transport of individual particles, and mass transport processes for conservative and non-conservative constituents, including salts, water temperature, dissolved oxygen, and dissolved organic carbon. We use DSM2 since there are not enough USGS sensor stations in the area of interest to obtain boundary conditions and additional flow measurements needed for the data assimilation. DSM2 is one of the reference models used by the DWR for operations and will be considered in this work as the ground truth.

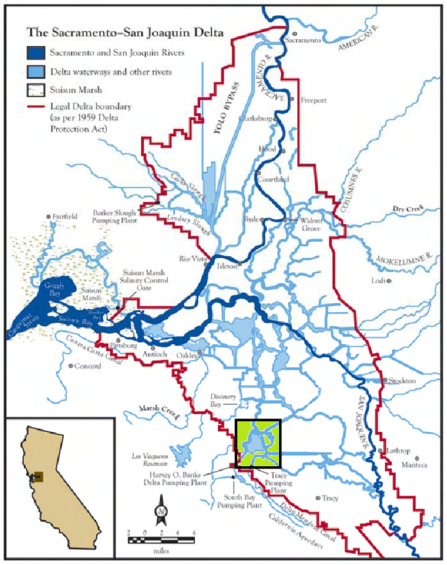

Fig. 3: The Sacramento-San Joaquin Delta, image adapted from [26]. The small box on the southern part of the Delta is the network considered for implementation in the current article.

A. *Numerical results*

We perform an experiment for a period of 25 hours using historical data corresponding to June 12, 2006. We obtain the boundary conditions and measurements used for data assimilation from DSM2. As boundary conditions, discharge is imposed at nodes 1, 7, 15, 16 and 17 and stage is imposed at nodes 4 and 12.

The number of cells in each subchannel is chosen in a way that the spatial step size in the subchannel is close to and not smaller than 900 ft and the temporal step size is chosen to be 15 sec. This choice of spatial step size results in 204 cells for the full network. Since at each internal cell, there are two states, discharge and stage, and there is one state at the boundary cells, we will have a 401 dimensional system. We run DSM2 with spatial step size of 5,000 ft and temporal step size of 15 min. We run DSM2 starting one day earlier so that the effects of inaccurate initial conditions are washed away and the DSM2 results are close to reality from the beginning of the experiment.

To perform data assimilation, we only assimilate discharge

(a)

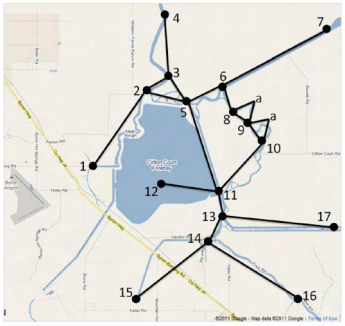

(b)

Fig. 4: (a) Satellite image of the channel network around the Clifton Court Forebay used for the experiment. (b) The network connectivity of the channel network used for the experiment consisiting of 19 subchannels, 10 junctions and one reservoir.

as the stage results computed by the forward simulation are relatively close to the corresponding results of DSM2. We use six discharge measurements at the middle of channels 3-4, 6-8, 9a10, 10-11, 5-11, 13-14. The process and measurement noises are assumed to be zero-mean white Gaussian noise. We assume that the noise on different measurements are uncorrelated. At each cell, the process noise on discharge is assumed to be correlated with the discharge at its four neighboring cells from each side. The variance on discharge at each cell is taken to be 25 and the correlations are taken to be 20, 12, 8, 4 with the discharge at the neighboring cells, respectively. The sensor measurements are obtained from DSM2 and a zero-mean Gaussian noise with a variance of 50 is added to these measurements to simulate the uncertainty in the measurements.

Using these flow measurements, the optimal SIR filter is applied. Figure 5 shows the results of the forward simulation and the SIR filter with 1000 particles compared to the corresponding results obtained from DSM2. The discharge at four locations in the network are illustrated for the period of the experiment. As can be seen in this figure, the SIR filter improves the model results significantly. In order to quantify the performance of the methods more rigorously, we calculate the relative error throughout the whole domain at each time step using the following formula

$$E(k) = \sqrt{\frac{\sum_{i=1}^{N_{\text{cells}}} (\hat{Q}_i^k - Q_i^k)^2}{\sum_{i=1}^{N_{\text{cells}}} (Q_i^k)^2}} \qquad (32)$$

where Q_i^k and $\hat{Q}_i^k$ are the true value of the flow and the estimated flow at cell i and time step k, respectively.

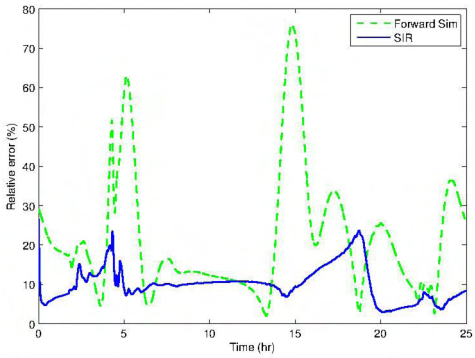

Fig. 6: Time evolution of relative error for forward simulation and the optimal SIR filter.

In Table II, the average relative error per time step is provided for the forward simulation and the optimal SIR for a few different number of particles. As can be seen in this table, performing data assimilation using the optimal SIR filter reduces the average error of the model from about 23% to around 10% which is a significant improvement.

TABLE II: Average Relative error corresponding to the forward simulation and the optimal SIR for a few different number of particles.

Method	Number of particles	Error(%): mean/variance
Forward sim.	-	23.36
SIR	1	10.87 / 0.63
SIR	10	10.41 / 0.48
SIR	100	10.28 / 0.39
SIR	1000	10.15 / 0.30

V. CONCLUSION

We investigated the performance of the *optimal importance resampling filter*, applied for estimation of water flow in an open channel network consisting of 19 subchannels and one reservoir in Sacramento-San Joaquin Delta in California. Starting from one-dimensional Saint-Venant equations, we constructed a state-space model of the flow in the network of interest. Considering a case in which additional measurements of the flow are available, we implemented the optimal sequential importance resampling filter and the numerical results were presented.

Applying other sequential Monte Carlo methods, e.g. Ensemble Kalman Filter and the recently developed implicit particle filter, to perform the data assimilation and comparing the performance of these methods is a topic of future work.

VI. ACKNOWLEDGEMENTS

We would like to thank Professor Alexander Chorin and Mathias Morzfeld with the Mathematics department at UC-Berkeley for fruitful discussions about particle filters and their useful suggestions and comments about the implementation.

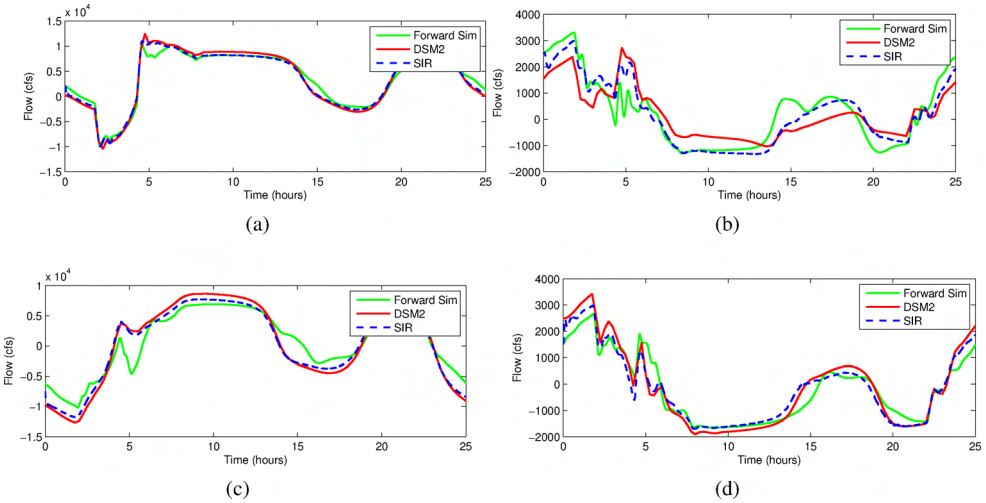

Fig. 5: Time evolution of discharge at six channels in the network, (a) channel 11-13 (b) channel 5-6 (c) channel 3-4 (d) channel 2-5, obtained from the forward simulation and the optimal SIR filter compared with the ground truth, i.e. DSM2 results.

REFERENCES

[1] P. Brasseur and J.C.J. Nihoul . Data assimilation: Tools for modelling the ocean in a global change perspective. *In NATO ASI Series, Series I: Global Environmental Change*, 19(239), 1994.

[2] J.A Cunge, F.M. Holly, and A. Verwey. *Practical aspects of computational river hydraulics*. Pitman, 1980.

[3] D.B. Haidvogel and A.R. Robinson . Special issue on data assimilation. *Dyn. Atmos. Oceans*, 13:171–517, 1989.

[4] P. Malanotte-Rizzoli. Modern approaches to data assimilation in ocean modeling. *Elsevier Oceanography Series*, 1996.

[5] I.M. Navon. Practical and theoretical aspects of adjoint parameter estimation and identifiability in meteorology and oceanography. *Dyn. Atmos. Oceans*, (27), 1997.

[6] B.D.O. Anderson and J.B. Moore. *Optimal Filtering*. Prentice-Hall, 1979.

[7] M. Arulampalam, S. Maskell, N. Gordon, and T. Clapp. A tutorial on particl filters for online nonlinear/non-gaussian baysian tracking. *IEEE Transactions on Signal Processing*, 50(2):174–188, 2002.

[8] N. Bergman. *Recursive Baysian Estimation: Navigation and Tracking applications*. PhD Dissertation, Linkoping University, Linkoping, Sweden, 1999.

[9] J. Carpenter, P. Clifford, and P. Fearnhead. Improved particle filter for nonlinear problems. *Proc. Inst. Elec. Eng., Radar, Sonar, Navig.*, 1999.

[10] M.H. Chaudhry. *Open-Channel Flow*. Springer, 2008.

[11] V. Chow. *Open-channel Hydraulics*. McGraw-Hill Book Company, New York NY, 1988.

[12] P. Del Moral. Measure valued processes and interacting particle systems. application to nonlinear filtering problems. *Ann. Appl. Probab.*, 1998.

[13] A. Doucet, N. de Freitas, and editors N. Gordon. *Sequential Monte Carlo Methods in Practice*. Springer-Verlag, 2001.

[14] A. Doucet, S. Godsil, and C. Andrieu. On sequential monte carlo methods for baysian filtering. *Statistics and Computing*, 2000.

[15] G. Evensen. *Data Assimilation: The Ensemble Kalman Filter*. Springer-Verlag, 2007.

[16] N. J. Gordon, D. J Salmond, A. F. M. Smith, and T. Clapp. Novel approach to nonlinear/non-gaussian baysian state estimation. *Radar and Signal Processing, IEE Proceedings F*, 140(2):107–113, 1993.

[17] S.S. Haykin. ***Kalman filtering and neural networks***. John Wiley & Sons Inc., 2001.

[18] Y. Ishikawa, T. Awaji, K. Akitomo, and B. Qiu. Successive correction of the mean sea surface height by the simultaneous assimilation of drifting buoy and altimetric data. *J. Phys. Oceanogr.*, (26):2381–2397, 1996.

[19] S.J. Julier and J.K. Uhlmann. A new extension of the kalman filter to nonlinear systems. In *Proc. of AeroSense: The 11th Int. Symp. on Aerospace/Defense Sensing, Simulations and Controls*, 1997.

[20] R.E. Kalman. A new approach to linear filtering and prediction problems1. *Journal of Basic Engineering*, 1960.

[21] E. Kalnay. *Atmospheric Modeling, Data Assimilation and Predictability*. Cambridge University Press, 2003.

[22] G. Kitagawa. Monte carlo filter and smoother for non-gaussian nonlinear state space models. *Journal of Comput. Graph. Statist.*, 5(1):1–25, 1996.

[23] L. Kuznetsov, K. Ide, and C.K.R.T. Jones. A method for assimilation of lagrangian data. *Mon. Wea. Rev.*, 131(10):2247–2260, 2003.

[24] X. Litrico and V. Fromion. *Modeling and Control of Hydrosystems*. Springer, 2009.

[25] S. Liu and R. Chen. Sequential monte carlo methods for dynamic systems. *Journal of the American Statistical Association*, 93(443):1032–1044, 1998.

[26] J. Lund, E. Hanak, W. Fleenor, R. Howitt, J. Mount, and P. Moyle. *Envisioning futures for the Sacramento-San Joaquin Delta*. 2007.

[27] A. Molcard, L.I. Piterbarg, A. Griffa, T. Ozgokmen, and A. Mariano. Assimilation of drifter observations for the reconstruction of the eulerian circulation field. *J. Geophys. Res.*, 108(C3), 2003.

[28] H. Moradkhani, K.L. Hsu, H. Gupta, and S. Sorooshian. Uncertainty assessment of hydrologic model states and parameters: Sequential data assimilation using the particle filter. *Water Resources Research*, 41, 2005.

[29] C. Paniconi, M. Marrocu, M. Putti, and M. Verbunt. Newtonian nudging for a richards equation-based distributed hydrological model. *Adv. Water. Resour.*, 26(2):161–178, 1996.

[30] T.W. Strum. *Open Channel Hydraulics*. McGraw-Hill, 2001.

[31] P. van Leeuwen. Nonlinear data assimilation in geosciences: An extremely efficient particle filter. *Quart. J. Roy. Meteo. Soc.*, 136:1991–1999, 2010.

[32] E.A. Wan and R. van der Merwe. The unscented kalman filter for nonlinear estimation. In *Proc. of the IEEE Symp. on Adaptive Systems for Signal Processing, Communication and Control (AS-SPCC)*, Lake Louise, Alberta, Canada, 2000.

[33] D. Wang, Y. Chen, and X. Cai. State and parameter estimation of hydrologic models using the constrained ensemble kalman filter. *Water Resources Research*, 45, 2009.

[34] J. Weare. Particle filtering with path sampling and an application to a bimodal ocean current model. *J. Comp. Phys.*, 228:4312–4331, 2009.